Journal of Artificial Intelligence Practice (2022)
Clausius Scientific Press, Canada

DOI: 10.23977/jaip.2022.050116
ISSN 2371-8412 Vol. 5 Num. 1

Overview of Sensorless Zero-Low Speed Range Control Technology based on High-Frequency Signal Injection for SPMSM

Duquan Zuo[1,2,3,a,*], Jie Liu[1], Huifang Li[3,b,*], Tao Wang[3], Yingjie Li[3]

[1]*Aviation Engineering College, Civil Aviation Flight University of China, Guanghan, 618307, People's Republic of China*
[2]*College of Mechanical Engineering, Chongqing Three Gorges University, Chongqing, 404100, People's Republic of China*
[3]*Huzhou Yueqiu Motor Co., Ltd., Huzhou, 313009, People's Republic of China,*
[a]*taiyanghefeng@cafuc.edu.cn;* [b]*li.huifang@yqmotor.com*
[*]*Corresponding author*

Keywords: PMSM; Sensorless; High frequency signal injection; Zero-Low Speed Range; Rotor position estimation

Abstract: For the sensorless position control technology of surface permanent magnet synchronous motor (SPMSM) under the operation modes of zero and low speed, this paper introduced several typical control algorithms detecting rotor position of PMSM, and analyzed the working principle and the rotor position estimation deviation control process of these types of algorithms, as well as their advantages and disadvantages in detail. Finally, the applicability of these algorithms in SPMSM at present were further compared and summarized, so as to achieve better control effect.

1. Introduction

New energy electric vehicle is the new mainstream of current vehicle development. With the rapid development of motor control theory, power transmission technology and permanent magnet materials, PMSM has become a research hotspot of air conditioning compressor driven of high-performance electric vehicle [1-2]. Compared with other motors, PMSM used sensors (canceling commutator and brush) to generate reversing signal has significant advantages such as light structure, simple control system, low vibration and noise, high power factor, fast response speed and transmission efficiency. PMSM is essentially a nonlinear coupled time-varying system [3]. Although the vector control method can realize high dynamic response, high dynamic and static accuracy and wide range speed regulation of the mentioned system, and is not sensitive to parameter changes and disturbances, it is inevitable to obtain the rotor position in real time [4].

The performance and detection accuracy of traditional mechanical sensors are easy to be reduced due to environmental impact and the installation concentricity problem, as well as the volume and cost of the installation interface or wiring are easy to be increased. Thus, in order to achieve the purpose of replacing mechanical sensors with sensorless control algorithm and realizing accurate speed regulation of motor, it is particularly necessary to carry out the research on sensorless control strategy with high precision, reliable performance and low cost. According to the estimation effect of motor rotor position and speed information in the full speed range, the PMSM sensorless control strategy can be divided into two categories: medium-high speed range and zero-low speed range [5]. The speed control driven system in medium-high speed range mainly adopts flux-linkage observation method, model reference adaptive method and back electromotive force (BEMF) to dynamically capture the rotor position of PMSM, these method is not enough to accurately estimate the rotor position and speed because the BEMF in zero-low speed range is smaller, the stator voltage is lower and the observed signal-to-noise ratio is larger. However, the high-frequency signal injection method can track the salient pole position well, and achieve the purpose of accurate detection for the position and speed information of sensorless control method in low-speed or even zero speed range [6].

Because the electric vehicle is propelled by high-power electric power, the signal-to-noise ratio control of useful signals has very high requirements when the motor runs in the zero-low speed range. In order to achieve the optimal efficiency mode with high signal-to-noise ratio and high torque ripple under vector control, the current research focus is on the the control algorithm and initial position estimation for the rotor angle of PMSM under zero-low speed operation mode. At present, the estimation algorithms for detecting rotor position information based on the high-frequency signal response of salient pole model have the high-frequency rotating voltage injection method, high-frequency pulse voltage injection method and high-frequency square wave voltage injection method [7]. In view of this, in this paper, the control method of surface permanent magnet synchronous motor (SPMSM) is selected as the object. Each algorithm is described and analyzed, and then, the rotor position estimation of the motor is analyzed and summarized.

2. Method comparison for zero-low speed range

Due to its simple implementation process, insensitive to the change of motor parameters and good sensorless tracking effect of motor rotor position, the high frequency voltage injection method based on salient pole model is widely used in the sensorless control system of zero-low speed operation.

2.1 High-frequency rotating voltage injection method

The basic principle of the high-frequency rotating voltage injection method for estimating the rotor position and velocity information is shown in Figure 1a. The high-frequency rotating voltage is injected into the α-β two-phase stationary coordinate system with cosine voltage and sinusoidal voltage (see Eq. 1). The voltage vector rotates under the action of internal asymmetry of the motor and generates high-frequency current response (see Eq. 2). The filter is used to extract the rotor angle information through filtering, demodulation and coordinate transformation of the response current (see Eq. 3), and the rotor position estimation error can then be obtained. At the same time, the position tracking observer is used to adjust the position deviation to zero [9-10] by phase-locked loop (PLL), and the actual position of the rotor can then be estimated (see Eq. 5).

$$u_j = \begin{bmatrix} u_{\alpha j} \\ u_{\beta j} \end{bmatrix} = V_j \begin{bmatrix} \cos w_h t \\ \sin w_h t \end{bmatrix} \quad (1)$$

Where u_j is the voltage vector; V_j is the voltage vector amplitude; w_h denotes voltage vector angular frequency; $\alpha-\beta$ represents the stationary coordinate system; $\hat{d}-\hat{q}$ represents the synchronous rotating coordinate system; θ and $\hat{\theta}$ are the actual and estimated positions of the rotor, respectively, θ_{err} denotes the estimated deviation of the above-mentioned positions. By introducing coordinate transformation $e^{j(-w_h t+\frac{\pi}{2})}$, the expression of high-frequency response current is:

$$\begin{cases} i_h e^{j(-w_h t+\frac{\pi}{2})} = I_{cn} e^{j(2\theta-2w_h t+\pi)} + I_{cp} \\ I_{cn} = V_j L_2 / w_h (L_1^2 - L_2^2),\ I_{cp} = V_j L_1 / w_h (L_1^2 - L_2^2) \end{cases} \quad (2)$$

Where i_h is the high-frequency current; L_1 denotes the mean inductance; L_2 denotes the difference inductance. It can be seen from equation (2) that the high frequency current transformed by coordinate is composed of DC component I_{cp} and rotating current vector $I_{cn} e^{j(2\theta-2w_h t+\pi)}$ containing rotor position information. After filtering and demodulation by high-pass filter, it can be expressed as follows:

$$HPF(i_h e^{j(-w_h t+\frac{\pi}{2})}) = I_{cn} e^{j(2\theta-2w_h t+\pi)} \quad (3)$$

The equation (3) is transformed by coordinate, one can obtain:

$$I_{cn} e^{j(2\theta-2w_h t+\pi)} e^{2j(w_h t)} = I_{cn} e^{j2\theta} \quad (4)$$

The filtering, demodulation and coordinate transformation processes of equations (2) to (4) are shown in Figure 1b, and the negative-sequence high-frequency current separated is presented in the following:

$$\begin{bmatrix} i_{\alpha n} \\ i_{\beta n} \end{bmatrix} = \begin{bmatrix} I_{cn} \cos 2\theta \\ I_{cn} \sin 2\theta \end{bmatrix} \quad (5)$$

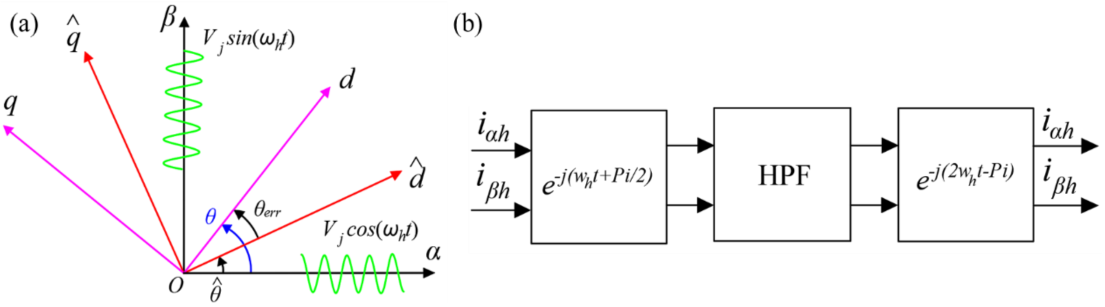

Figure 1. Schematic diagram of: (a) the high-frequency rotating voltage injection; (b) the signal processing for the high-pass filter.

The combined structure of PLL and position tracking observer is composed of phase discriminator, loop filter and PC oscillator, as shown in Figure 2.

In Figure 2, the observed rotor position is proposed by the phase discriminator, the high frequency and noise signals are removed by the loop filter, and the PC oscillator maintains I/O phase consistent. The high frequency currents $i_{\alpha n}$ and $i_{\beta n}$ are input to the α and β axes, and a trigonometric function containing position information is multiplied on both sides of the high frequency current. Then the rotor position error ε is represented as:

$$\varepsilon = I_{cn} \sin 2(\theta - \hat{\theta}) = I_{cn} \sin 2\theta_{err} \quad (6)$$

When θ_{err} is smaller, the equation (5) can be simplified as:

$$\varepsilon \approx 2 I_{cn} \theta_{err} \quad (7)$$

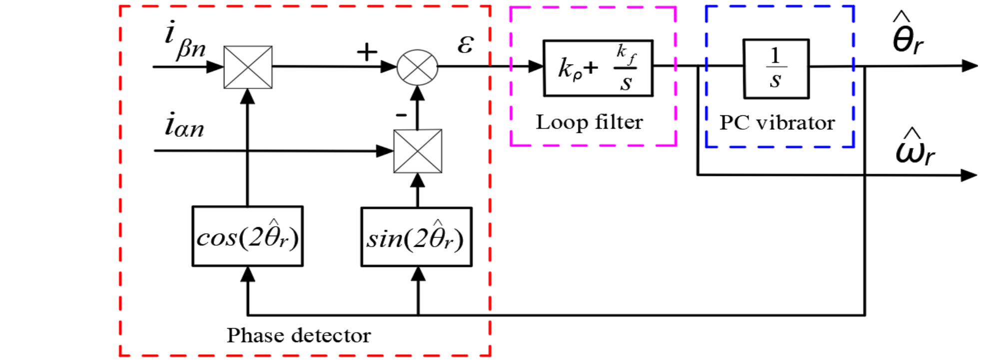

Figure 2. Combined structure of PLL and observer.

The key to the sensorless control technology of the high-frequency rotating voltage injection method is to use the phase-locked loop structure to make the estimation error θ_{err} closed-loop to 0, so as to ensure that the actual position angle θ of the rotor is equal to the estimated position angle $\hat{\theta}$ [11]. Figure 3 is the control system framework of high-frequency rotating voltage injection method. As can be seen from the figure 4, the multiple low-pass filters are used at the current loop and rotor position, which complicates the signal extraction process and aggravates the instability of the system.

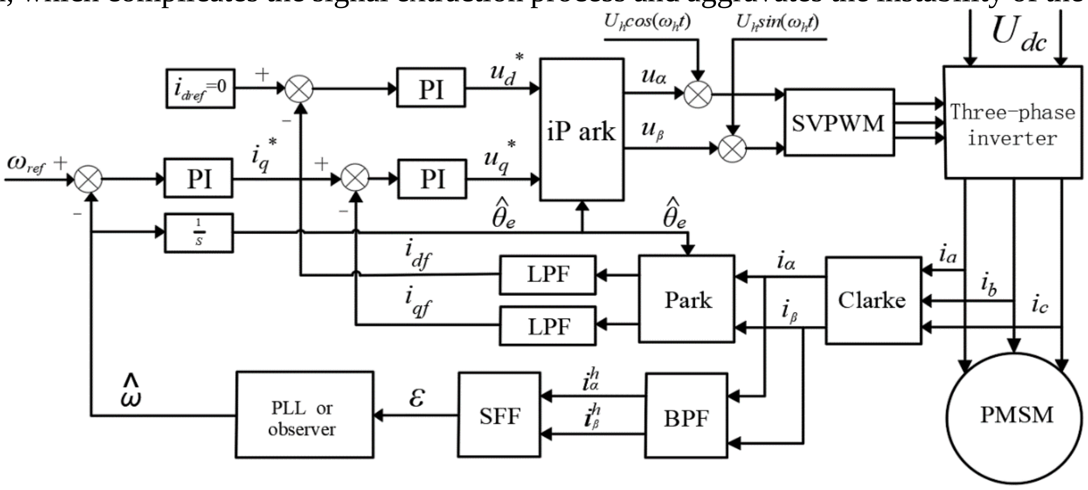

Figure 3. Control system of high-frequency rotating voltage injection method.

In sum, the implementation process of the high-frequency rotating voltage injection method is intuitive, the transient response characteristics are good, and it is not sensitive to the change of motor parameters. Therefore, the whole process shows good robustness. However, its shortcomings are that the application scope is narrow and it is not suitable for SPMSM, as well as the salient pole effect must be produced by the salient pole rotor structure inside the motor, which is only suitable for the interior permanent magnet synchronous motor (IPMSM) with salient pole ratio. In addition, the manufacturing process is complex, and the introduced filter will make the system phase delay.

2.2 High-frequency pulsating voltage injection method

The high-frequency pulsating voltage injection method is shown in Figure 4a. The high-frequency pulse voltage (sinusoidal signal) is injected into the $\hat{d}$ axis of the synchronous rotating coordinate system ($\hat{d}-\hat{q}$), and then the corresponding voltage signal is described as:

$$u_j = \begin{bmatrix} u_{dj} \\ u_{qj} \end{bmatrix} = \begin{bmatrix} V_j \cos w_h t \\ 0 \end{bmatrix} (8)$$

Where *d-q* and $\hat{d} - \hat{q}$ are the actual and estimated synchronous rotating coordinate systems, respectively.

Under the coupling effect of rotor magnetic field and high-frequency pulsating magnetic field generated by stator, the saturation state of D-axis excitation magnetic circuit will produce salient pole saturation effect [12]. At the same time, the estimation error of rotor between the estimated position and the actual position is obtained by demodulating and filtering the high-frequency current extracted from the $\hat{q}$ axis, which is used as the input of PLL and the position tracking observer, and the position error is adjusted to zero by using the regulator, so the real position of the rotor can be obtained. Combining equations (2) and (8), the high-frequency response current in the coordinate system $\hat{d} - \hat{q}$ is presented by equation (9):

$$\begin{bmatrix} \hat{i}_d \\ \hat{i}_q \end{bmatrix} = \begin{bmatrix} I_{cn} \cos 2\theta_{err} + I_{cp} \\ I_{cn} \sin 2\theta_{err} \end{bmatrix} \sin w_h t \ (9)$$

It can be seen from equation (9) that when the high-frequency signal is smaller and can be ignored, the high-frequency current of $\hat{d}$ axis is the sum of cosine quantity and direct variables, and the high frequency current of $\hat{q}$ axis is sinusoidal quantity. When the actual position θ is close to the estimated position $\hat{\theta}$ ($\theta_{err} \to 0$), the existing relationship is as follows:

$$\hat{i}_d \to I_{cn} + I_{cp},\ \hat{i}_q \to 0 \ (10)$$

In equation (10), it can be seen that the rotor position extraction of SPMSM can be estimated by the standard that the $\hat{q}$ axis high-frequency response current converges to zero. The coordinate transformation $\sin w_h t$ is introduced to the high-frequency current of $\hat{q}$ axis, and the high-frequency component $2w_h t$ is filter out by the low-pass filter (see Figure 4b). Then the equation (9) is modified as follows:

$$LPF(\hat{i}_q \sin w_h t) = \frac{1}{2} I_{cn} \sin 2\theta_{err} \ (11)$$

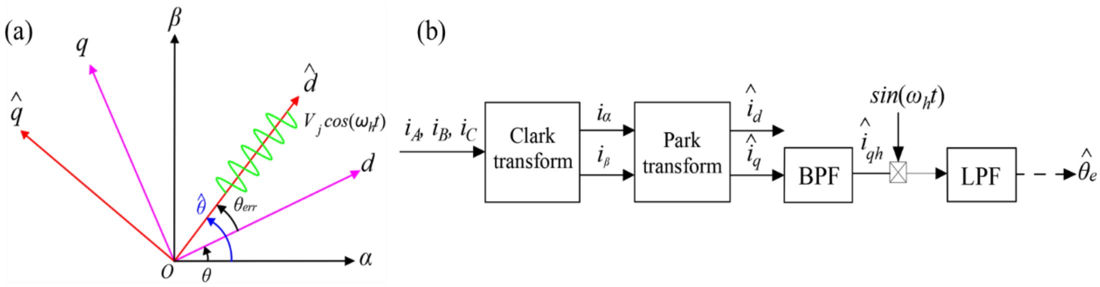

Figure 4. Schematic diagram of: (a) the high-frequency pulsating voltage injection; (b) the extraction process for rotor position information.

It can be seen from equation (11) that when the estimated deviation θ_{err} of between $\hat{\theta}$ and θ approaches 0, $I_{cn} \sin 2\theta_{err}$ is also close to 0, the rotor position tracking can be realized through the estimation deviation of the two positions mentioned above. Figure 5 is the frame of the sensorless control system adopted the high-frequency pulsating voltage injection. It can be seen that the PLL structure introduces PI regulator control, and the corresponding rotor position estimation deviation ε is approximately equal to $I_{cn}\theta_{err}$.

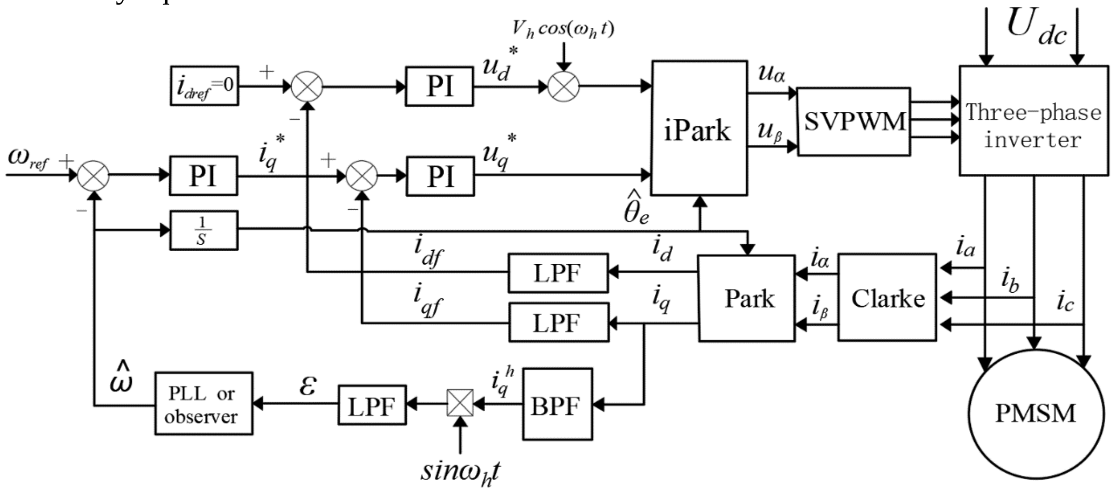

Figure 5. Control system of high-frequency pulsating voltage injection method.

2.3 High-frequency square wave voltage injection method

The high-frequency square wave voltage injection method is the same as the high-frequency pulsating voltage injection method, and the difference is that the injection voltage of the former is a square wave signal [14], as shown in figure 6a. It increases the injection frequency to PWM frequency which is higher than that of the pulsating voltage injection method. The low-pass filter is not used in the separation process of high frequency current and fundamental frequency current, which improves the closed-loop bandwidth and dynamic response performance of the system current, and is more suitable for SPMSM. The mentioned injection method is to inject high-frequency square wave voltage signal on the $\hat{d}$ axis of synchronous rotating coordinate system ($\hat{d}-\hat{q}$) (see Eq. 12), and the injected voltage amplitude is consistent with the change of PWM period, as shown in figure 6b.

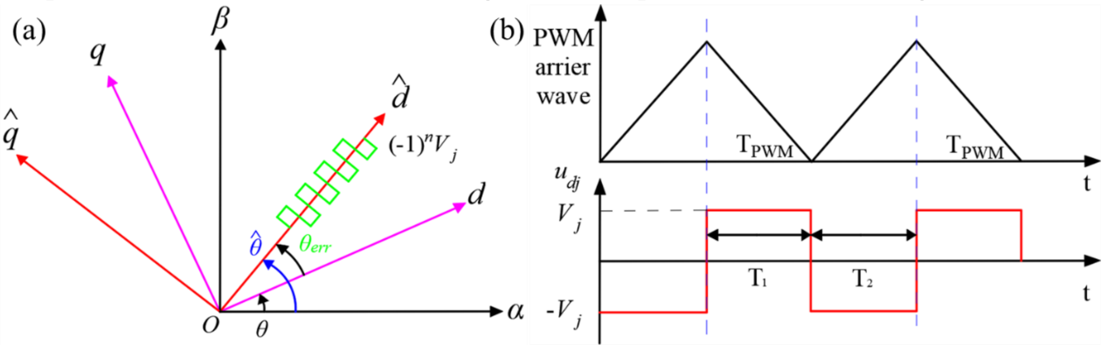

Figure 6. Schematic diagram of: (a) the high-frequency pulsating voltage injection; (b) the extraction process for rotor position information.

Combined with PMSM high-frequency mathematical model [15-16], the high-frequency response current in $\hat{d}-\hat{q}$ coordinate system can be rewritten as follows:

$$\begin{bmatrix} \Delta i_d^h \\ \Delta i_q^h \end{bmatrix} = K \begin{bmatrix} L_d \cos^2 \theta_{err} + L_q \sin^2 \theta_{err} \\ (L_d - L_q)/2 \sin 2\theta_{err} \end{bmatrix} \tag{13}$$

Where K equals to $(-1)^n V_j \Delta T / L_d L_q$; Δi^h denotes the high-frequency response current; ΔT denotes the injection voltage variation period. It can be seen from equation (13) that the high-frequency current of $\hat{d}$ axis is the sum of cosine and sinusoidal quantities, and the high-frequency current of $\hat{q}$ axis is the sinusoidal quantity. The rotor position estimation error is only included in the high-frequency current of $\hat{q}$ axis. When the estimated position θ is close to the actual position $\hat{\theta}$ ($\theta_{err} \to 0$), the position estimation error of $\hat{q}$ axis is extracted, and there is:

$$\theta_{err} = \frac{L_d L_q \Delta i_q^h}{(-1)^n V_j \Delta T (L_d - L_q)} \quad (14)$$

The high-frequency square-wave voltage signal based on the PWM period is the positive and negative symmetry, and the sampling current response only in the adjacent period is used, the magnitude of response current above-mentioned is equal but its amplitude is opposite. Thus, the size and direction of the separated fundamental frequency and high frequency currents do not change which avoid the use of low-pass and band-pass filters, and then the current closed-loop bandwidth is improved, so the purpose of improving the dynamic response and steady-state performance of the sensorless control system is ultimately achieved. The schematic diagram of the rotor position extraction of the sensor control system with the high-frequency square-wave voltage injection method without filters is presented in Figure 7.

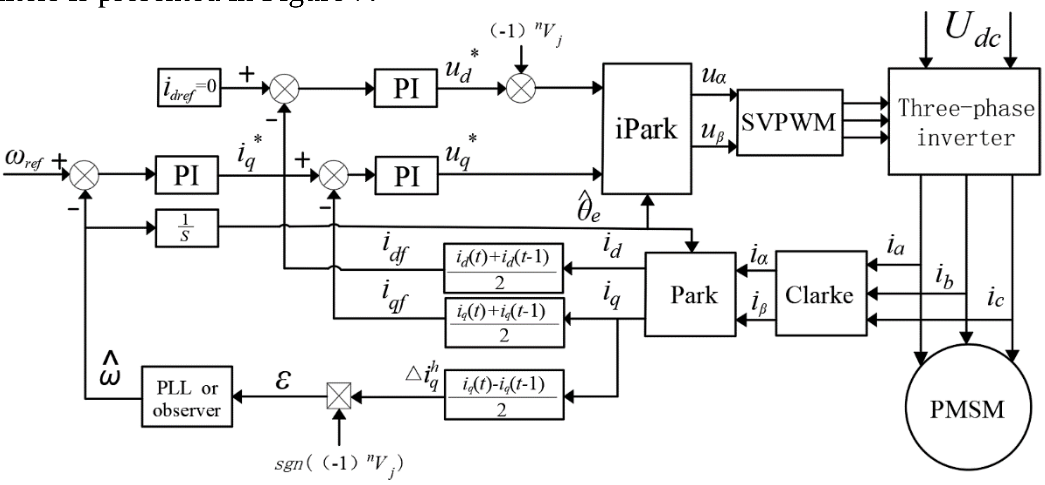

Figure 7. Control system of high-frequency square wave voltage injection method.

3. Summary of methods applicable to zero-low speed range

High-frequency signal injection is one of the most widely used zero-low speed sensorless control methods. From the above analysis, it can be concluded that the lowest frequency of high-frequency voltage signal injection is closely related to the fundamental frequency. When the injection frequency is too low, the positioning error will be caused by the minimal rotation of the motor rotor. And when the injection frequency is close to the fundamental frequency, the detection accuracy will be affected by the difficulty of separating the two kinds of frequencies mentioned above. Taking the injected square-wave signal as an example, when the maximum frequency of the injected signal reaches the PWM carrier frequency, the continuous injection will increase the equivalent inductances L_d and L_q of the synchronous rotating coordinate system, which will further reduce the high-frequency current under the same voltage signal injection and make it difficult to extract the rotor position information.

Therefore, to ensure the signal-to-noise ratio and accuracy of the rotor position sensorless control system at zero-low speed range, the injection frequency of motor needs to select the appropriate range.

4. Conclusion

In this paper, three algorithms of PMSM sensorless control system in zero-low speed range are introduced, and the working principle of each method, the control process of estimation deviation for rotor position, the corresponding advantages and disadvantages are analyzed and summarized. The conclusions are as follows:

(1) The high-frequency rotating voltage injection method needs to inject high-frequency cosine and sinusoidal signals at the same time. The injection of the latter will form a high-frequency rotating magnetomotive force in space, resulting in being constant 0 for the rotor position estimation deviation, which is not suitable for SPMSM. It is only suitable for IPMSM with significant salient pole effect, and the excessive use of filters will also cause phase delays in systems. However, the implementation process of this method is intuitive, insensitive to changes in motor parameters, and has good system robustness.

(2) The advantages of high-frequency pulsating voltage injection method are that only high-frequency sinusoidal voltage signal is injected and the process is greatly simplified, which is suitable for SPMSM and IPMSM. Although the number of low-pass filters in the system is significantly less than that of high-frequency rotating injection method, it still causes problems such as phase delay, current loop bandwidth reduction and initial position non-convergence.

(3) The injection frequency of the high-frequency square-wave voltage injection method can fully approximate or even reach the PWM frequency. The high-frequency current and the fundamental current can be separated without the filter, so as to ensure the steady-state performance and the dynamic response performance of the sensorless control system.

In a word, the high-frequency square-wave voltage injection method has better application effect than the other two kinds of injection methods in SPMSM.

Acknowledgements

This work was supported by China Postdoctoral Science Foundation (No. 2021m673227), by general project of Chongqing Natural Science Foundation (No. cstc2021jcyj-msxmX0072), by project of science and technology research program of Chongqing Education Commission of China (No. KJQN202101202), and by Chongqing Engineering Research Center for Advanced Intelligent Manufacturing Technology under contract number ZNZZXDJS202002, Research Department of Chongqing, China.

References

[1] YC Song, SQ Guo. Permanent magnet synchronous motor control strategy for electric vehicle [J]. Internal Combustion Engine & Parts, 2022(1): 62-64.

[2] Q Chen, Y, Tian, S Kang, et al. Sensorless control of permanent magnet synchronous motor for electric vehicle based on phase locked loop[J]. International Journal of Automotive Technology, 2021, 22(5): 1409-1414.

[3] R Sakthivel, S Santra, B Kaviarasan, et al. Finite-time sampled-data control of permanent magnet synchronous motor systems[J]. Nonlinear Dynamics, 2016, 86(3): 2081-2092.

[4]HY Hu, CX Cai, YJ Chen, et al. Research on permanent magnet synchronous motor vector control based on load feedforward compensation [J]. Micromotors, 2021, 54(1): 89-92.

[5] ZB Liu, JX Zhao, LL Zhou. A sensorless control method for permanent magnet synchronous motor in full speed range [P]. CN2020116294176, 2021-12-31.

[6] Z Zhang, C Hu, Y Zhang, et al. Research on High Frequency Voltage Injection Method for PMSM [C]. Industrial Electronics and Applications (ICIEA) 2019 14th IEEE Conference on, 18993258, 2019.

[7] F Qin. Research on sensorless control of PMSM based on the concept of power electronic system integration [D].

Zhejiang University, 2006.
[8] QH Wu, CX Huang, YX Hou. Sensorless FOC of PMSM based on high frequency square-wave voltage injection and improved luenberger position observer [J]. Journal of Electrical Engineering, 2021, 16(4): 120-126.
[9] DQ Zuo, LX Qian, TE Yang, et al. Coupling Leveling Control Based on Fuzzy PID for Synchronous Loading System of Load-Bearing Test Bed [J]. Chinese Journal of Electronics, 2017(06):1206-1212.
[10] B Shuang, ZQ Zhu. A novel method for estimating the high frequency incremental DQ-axis and cross-coupling inductances in interior permanent magnet synchronous machines [J]. IEEE Transactions on Industry Applications, 2021, 99: 4913-4923.
[11] C GU, XL Wang, ZQ Deng. A rotor position estimated error correction method for high-speed permanent magnet Synchronous motor based on dual-phase-locked-loop [J]. Proceedings of the CSEE, 2020, 40(3):962-969.
[12] S Liang, GY Liu. High frequency sinusoidal pulse voltage injection based sensorless control strategy for IPMSMs [J]. Micromotors, 2020, 53(4): 54-59.
[13] Wang Z X, Lin H C, Lu B F, et al. Experimental research of PMSM salient characteristic using pulsating high-frequency voltage injection [J]. Electric Machines & Control, 2015, 19(3): 19-24.
[14] JP Zhao, W Cui. Research of Sensorless Control for IPMSM Based on High-Frequency Square-Wave Voltage Injection Method [J]. Small & Special Electrical Machines, 2018, 46(4): 40-45.
[15] DQ Zuo, LX Qian, GF Xia, et al. Hydraulic leveling design and experimental research of an AMESim-based synchronous loading system for bearing test bed [J]. Chinese Journal of Applied Mechanics, 2019, 36(6): 1451-1456.
[16] A Rahimi, K Kanzi. High-frequency modelling of permanent magnet synchronous motor for conducted EMI studies [J]. IET Electric Power Applications, 2020(3): 110-119.